

ARTICLES

An SCN9A channelopathy causes congenital inability to experience pain

James J. Cox^{1*}, Frank Reimann^{2*}, Adeline K. Nicholas¹, Gemma Thornton¹, Emma Roberts³, Kelly Springell³, Gulshan Karbani⁴, Hussain Jafri⁵, Jovaria Mannan⁶, Yasmin Raashid⁷, Lihadh Al-Gazali⁸, Henan Hamamy⁹, Enza Maria Valente¹⁰, Shaun Gorman¹¹, Richard Williams¹², Duncan P. McHale¹², John N. Wood¹³, Fiona M. Gribble² & C. Geoffrey Woods¹

The complete inability to sense pain in an otherwise healthy individual is a very rare phenotype. In three consanguineous families from northern Pakistan, we mapped the condition as an autosomal-recessive trait to chromosome 2q24.3. This region contains the gene *SCN9A*, encoding the α -subunit of the voltage-gated sodium channel, $\text{Na}_v1.7$, which is strongly expressed in nociceptive neurons. Sequence analysis of *SCN9A* in affected individuals revealed three distinct homozygous nonsense mutations (S459X, I767X and W897X). We show that these mutations cause loss of function of $\text{Na}_v1.7$ by co-expression of wild-type or mutant human $\text{Na}_v1.7$ with sodium channel β_1 and β_2 subunits in HEK293 cells. In cells expressing mutant $\text{Na}_v1.7$, the currents were no greater than background. Our data suggest that *SCN9A* is an essential and non-redundant requirement for nociception in humans. These findings should stimulate the search for novel analgesics that selectively target this sodium channel subunit.

Pain is an essential sense that has evolved in all complex organisms to minimize tissue and cellular damage, and hence prolong survival. The onset of pain results in the adoption of behaviours that both remove the organism from a ‘dangerous environment’ and allow for tissue repair; for example, resting a broken limb so that new bone can form. Pain also protects us from our environment, by teaching us what situations and behaviours are likely to lead to injury. Pain pathways operate at numerous levels in the nervous system and are under both voluntary and involuntary control. Blockade of this system with analgesics has been a major pharmacological achievement.

Whereas individuals with a congenital absence of the sense of vision or of hearing are relatively common, a congenital absence of the sense of pain is very rare. The first case of a patient with a congenital inability to perceive pain was said to have been reported in the early twentieth century¹. Only a handful of such patients have since been described and are usually categorized as having ‘congenital indifference to pain’ (OMIM 243000, also known as autosomal recessive congenital analgesia) or as being misdiagnoses of ‘congenital insensitivity to pain’ (OMIM 608654, also known as hereditary sensory and autonomic neuropathy type 5 (HSAN5))^{2–4}. Historically these two conditions have been largely distinguished by the absence or presence, respectively, of an associated neuropathy². The existence of congenital indifference to pain has, however, been questioned and the nomenclature surrounding its differentiation from congenital insensitivity to pain has been the focus of controversy^{2,3,5} (see Methods). Here we describe individuals from three families with the extraordinary phenotype of a congenital inability to perceive any form of pain, in whom all other sensory modalities were preserved and the peripheral and central nervous systems were appar-

ently otherwise intact. As the clinical description of the study individuals does not exactly match pre-existing reports of either indifference to pain or insensitivity to pain, we refer to this new syndrome as ‘channelopathy-associated insensitivity to pain’ and show that it is caused by loss of function of the voltage-gated sodium channel gene *SCN9A*.

Absence of pain phenotype

The index case for the present study was a ten-year-old child, well known to the medical service after regularly performing ‘street theatre’. He placed knives through his arms and walked on burning coals, but experienced no pain. He died before being seen on his fourteenth birthday, after jumping off a house roof. Subsequently, we studied three further consanguineous families in which there were individuals with similar histories of a lack of pain appreciation, each originating from northern Pakistan and part of the Qureshi beldari/clan (Fig. 1). All six affected individuals had never felt any pain, at any time, in any part of their body. Even as babies they had shown no evidence of pain appreciation. None knew what pain felt like, although the older individuals realized what actions should elicit pain (including acting as if in pain after football tackles). All had injuries to their lips (some requiring later plastic surgery) and/or tongue (with loss of the distal third in two cases), caused by biting themselves in the first 4 yr of life. All had frequent bruises and cuts, and most had suffered fractures or osteomyelitis, which were only diagnosed in retrospect because of painless limping or lack of use of a limb. The children were considered of normal intelligence by their parents and teachers, and by the caring physicians. One author saw and reviewed all six affected individuals and their families. The ages at which the

¹Department of Medical Genetics, and ²Department of Clinical Biochemistry, Cambridge Institute for Medical Research, Wellcome/MRC Building, Addenbrooke's Hospital, Cambridge CB2 0XY, UK. ³Section of Ophthalmology and Neuroscience, Leeds Institute of Molecular Medicine, ⁴Department of Clinical Genetics, St James's University Hospital, Leeds LS9 7TF, UK. ⁵Gene Tech Lab 146/1, Shadman Jail Road, Lahore, Pakistan. ⁶Department of Paediatrics, Fatima Jinnah Medical College, Lahore, Pakistan. ⁷Department of Obstetrics and Gynaecology, King Edward Medical University, Lahore, Pakistan. ⁸Department of Paediatrics, Faculty of Medicine and Health Sciences, United Arab Emirates University, Al-Anin P O Box 15551, United Arab Emirates. ⁹National Center for Diabetes, Endocrinology and Genetics, Amman P O Box 3165/11942, Jordan. ¹⁰IRCCS CSS, San Giovanni Rotondo and CSS Mendel, Rome I-00168, Italy. ¹¹Department of Paediatrics, St Luke's Hospital, Bradford BD5 0NA, UK. ¹²Pfizer Global Research and Development, Sandwich Laboratories, Sandwich CT13 9NJ, UK. ¹³Molecular Nociception Group, Department of Biology, University College London, London WC1E 6BT, UK.

*These authors contributed equally to this work.

children were examined and their families initially seen were (with reference to Fig. 1 and from left to right): family 1, the children were 6, 4 and 14 years old; family 2, the child was 6 years old; and family 3, the children were 12 and 10 years old.

Detailed neurological examinations revealed that each could correctly perceive the sensations of touch, warm and cold temperature, proprioception, tickle and pressure, but not painful stimuli. Pain sensation was assessed by squeezing of the Achilles' tendon, firm pressure to dorsal fingertips inflicted with a thumbnail and by venesection; all were felt but not described as painful or unpleasant. Sensation of touch was assessed by needle point and cotton wool and was normal; proprioception was normal despite the children being 'ungainly' in gross motor movements; temperature sensation was not rigorously assessed but all children could tell cold from hot in food and drink (two had received painless scalds as young children). There was no evidence of a motor or sensory neuropathy. Strength, tone, reflexes including plantar responses, and appearance of joints were all normal. Peripheral nerves were not palpably enlarged. Corneal reflex was present, and the gag reflex was reported as normal. None had symptoms of autonomic nervous system dysfunction: all sweated and flushed/blushed appropriately; there were no increased episodes of hyperpyrexia (although these did occur appropriately with infection); tongues of all children were normal with no loss of fungiform papillae; bladder control occurred within the normal age spectrum and there was no history of urinary infections, incontinence or retention; there were no episodes of unexplained vomiting or dysphagia; tear production was reported as normal, and no child had dry eyes. However, a histamine flare test and assessment of itching

was not performed. All had normal health, vision, hearing and appearance.

Nerve conduction studies of the radial nerve were conducted in the older child in family 3 and the affected individual in family 2. The results were normal with no evidence of a neuropathy, either axonal or demyelinating. Nerve biopsy of the sural nerve was performed in the same two individuals and showed a normal sensory nerve with all nerve fibre types present, of normal morphology, and in normal distribution by light and electron microscopy. One member of family 1 had a magnetic resonance imaging (MRI) brain scan, which was reported and subsequently reviewed as showing no abnormalities. Parents and other siblings reported normal pain appreciation.

Mapping the disease gene

We used a positional cloning strategy to identify the mutated gene in these families (Fig. 1). A genome-wide scan using 400 polymorphic microsatellite markers led to the identification of an 11.7-megabase (Mb) homozygous region on chromosome 2q24 shared between the affected individuals from all three families. In order to reduce the region, we sought a common haplotype between families by genotyping an additional 73 polymorphic microsatellite markers (Supplementary Table 1). This analysis failed to identify a significant shared haplotype block, suggesting that each family had a different mutation. Bioinformatics analysis of the ~50 genes in the linkage region identified *SCN9A* as the best candidate gene, and subsequent sequence analysis of *SCN9A* revealed distinct homozygous nonsense mutations in each of the three families (Fig. 2 and Supplementary Table 2). In family 1 we found a single homozygous base substitution in coding exon 15 (2691G→A, resulting in the amino acid change W897X). In family 2 we found a single homozygous base deletion of

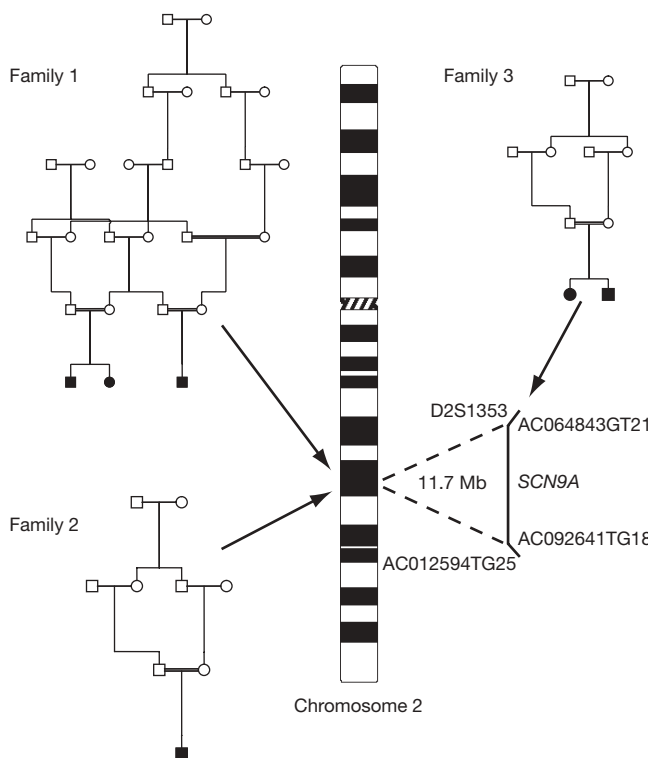


Figure 1 | The families used to map the locus for channelopathy-associated insensitivity to pain. Autozygosity mapping in families 1 and 2 on the left of the diagram enabled the identification of a shared 20 cM homozygous region on chromosome 2q24 (there were no other significant homozygous regions detected). The two-point LOD score was 3.2 at $\theta = 0$, for AC064843GT21 and AC092641TG18, but greater for more informative markers, see Supplementary Table 1. Family 3, on the right of the diagram, was used to refine this region to an 11.7-Mb shared homozygous region flanked by the heterozygous markers D2S1353 and AC012594TG25 and defined by the homozygous markers AC064843GT21 and AC092641TG18. Affected individuals are indicated with filled symbols.

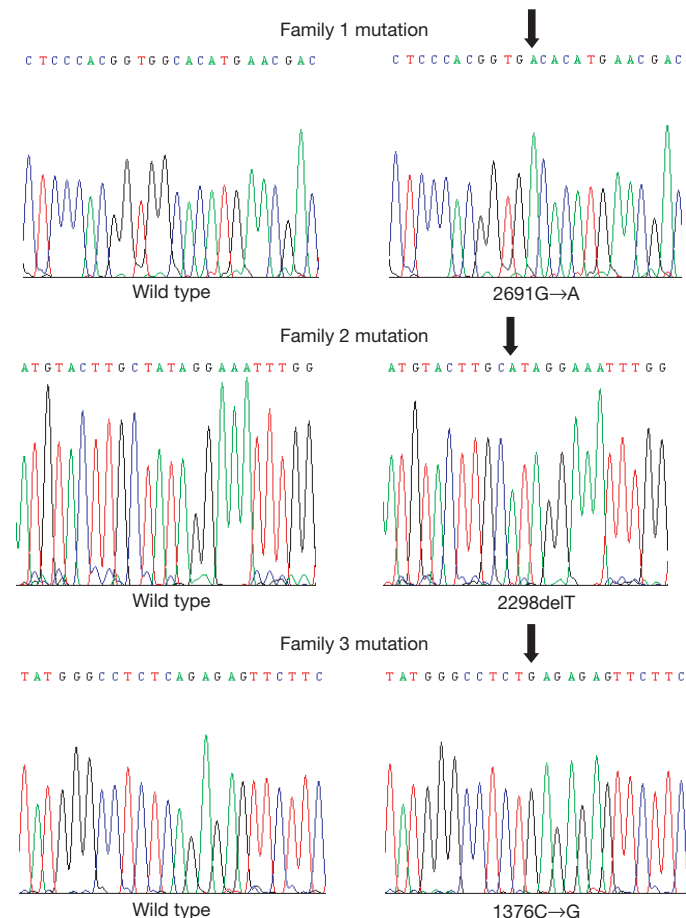


Figure 2 | Sequence chromatograms showing the mutations identified in families 1, 2 and 3. The arrows indicate the site of the mutations.

base 2298 in coding exon 13 that led to a frameshift and the amino acid change I767X. In family 3 we found a single homozygous base substitution in coding exon 10 (1376C→G, resulting in the amino acid change S459X) (Fig. 3). Each mutation was absent from 300 northern Pakistani control chromosomes and showed the expected disease segregation within the families. Although DNA was not available from the original index case, it is likely that he too had channelopathy-associated insensitivity to pain as his mother was heterozygous for the *SCN9A* nonsense mutation W897X (his father was not available to test). We considered the possibility that channelopathy-associated insensitivity to pain was inherited as a double recessive disorder in these families. However, we concluded that this was extremely unlikely because the 11.7-Mb region containing *SCN9A* was the only significant shared homozygous region between the three families and because the in-depth haplotype study of this linkage region (Supplementary Table 1) failed to identify a significant shared haplotype block.

SCN9A encodes $\text{Na}_v1.7$, the α -subunit of a tetrodotoxin-sensitive voltage-gated sodium channel that is expressed at high levels in peripheral sensory neurons, most notably in nociceptive small-diameter dorsal root ganglia (DRG) neurons^{6–8}. Voltage-gated sodium channels underlie the depolarizing phase of action potentials in excitable cells and tissue-specific expression of the various family members help to shape the excitability and repetitive firing properties of different neurons^{9,10}. The precise function of $\text{Na}_v1.7$ in sensory neurons is unclear, although immunostaining of cultured dorsal root ganglia neurons has suggested that it is targeted to the nerve terminals, where it has been proposed to have an involvement in action potential initiation^{7,11}.

Loss of function of $\text{Na}_v1.7$

The $\text{Na}_v1.7$ nonsense mutations identified in our families are expected to cause prematurely truncated proteins or nonsense-mediated messenger RNA decay and hence loss of function of $\text{Na}_v1.7$ in nociceptive neurons (Fig. 3)¹². To determine the activity of any possible stable truncated $\text{Na}_v1.7$ proteins, we carried out patch-clamp experiments in human embryonic kidney (HEK293) cells. Wild-type $\text{Na}_v1.7$, or $\text{Na}_v1.7$ containing the patient mutations, was co-expressed in HEK293 cells with the auxiliary sodium channel β_1 and β_2 subunits (encoded by *SCN1B* and *SCN2B*, respectively), which are also expressed in DRG neurons¹³ and are necessary for the normal function of voltage-gated sodium channels^{14,15}. We achieved this by the manufacture of two poly-cistronic constructs, allowing the independent expression of *SCN9A* (wild-type or mutant) and a red fluorescent protein, in addition to *SCN1B*, *SCN2B* and a green fluorescent protein (Fig. 4a). HEK293 cells were transiently transfected with both constructs using lipofection, and cells exhibiting

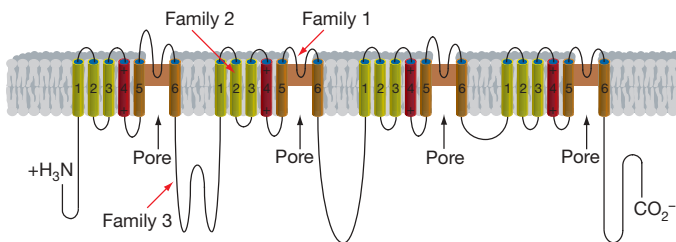


Figure 3 | Schematic representation of $\text{Na}_v1.7$, the voltage-gated sodium channel α -subunit encoded by *SCN9A*, and the locations of the identified human mutations. *SCN9A* encodes a plasma membrane protein: in the figure, the plasma membrane is shown in grey; the extracellular region is uppermost; and intracellular region below. $\text{Na}_v1.7$ is predicted to fold into four similar domains with each domain comprising six α -helical transmembrane segments (labelled 1–6). Transmembrane segments 5 and 6 are the pore-lining segments and the voltage sensor is located in transmembrane segment 4 of each domain (depicted by a plus symbol). The red arrows indicate the location of the nonsense mutation in each family.

both red and green fluorescence were selected for electrophysiological studies in the expectation that such cells would also express *SCN9A*, *SCN1B* and *SCN2B* (Fig. 4b). Control cells were transfected with the $\beta_1\beta_2$ subunit construct alone and selected on the basis of

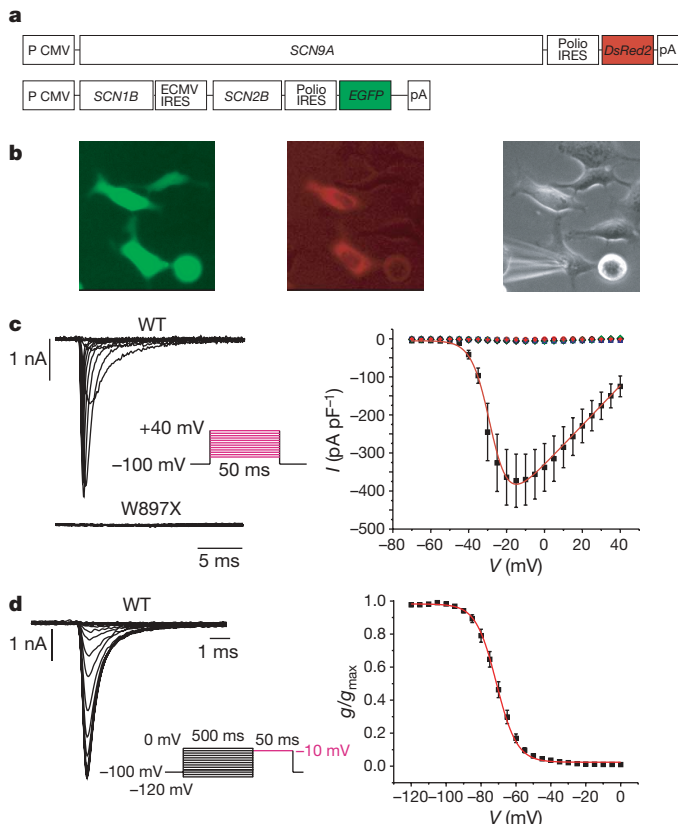


Figure 4 | Patch-clamping experiments to investigate the voltage-gated sodium channel activity of wild-type and truncated $\text{Na}_v1.7$. **a**, Constructs used in the patch-clamping experiments (see Supplementary Methods). We cloned wild-type *SCN9A* and then used site-directed mutagenesis to manufacture three further constructs each containing a family mutation. Each *SCN9A* construct was sequentially co-transfected with a plasmid containing the auxiliary sodium channel β_1 and β_2 subunits, and only cells clearly expressing DsRed2 (red fluorescence) and EGFP (green fluorescence) were measured for electrical activity. ECMV, encephalomyocarditis virus; IRES, internal ribosome entry site. **b**, A typical cell used in the patch-clamping experiments, showing both EGFP fluorescence (left) and DsRed2 fluorescence (middle), with the pipette attached in phase contrast (right). **c**, Left panel: initial current responses to 50-ms voltage steps of 5-mV increments between -70 and $+40$ mV from a holding potential of -100 mV, in a whole-cell voltage clamp recording applied at ~ 0.5 Hz for a cell co-expressing wild-type (WT) $\text{Na}_v1.7$ (top) or $\text{Na}_v1.7$ W897X (bottom) with the β -subunits. The inset shows the voltage pulse protocol. Right panel: current–voltage relationship of the peak currents normalized for cell size (pA per pF) obtained using the experimental set-up shown on the left. Black squares, wild type ($n = 13$); red circles, I767X ($n = 7$); blue squares, W897X ($n = 7$); green diamonds, S459X ($n = 5$); white diamonds, β -subunits only ($n = 5$). The red line represents a fit of the wild-type data with a Boltzmann equation $y = (A_2 + (A_1 - A_2)/(1 + \exp((V_{0.5} - x)/k)))(x - V_{rev})$, where $V_{0.5} = 28.0$ mV, $k = 4.9$ mV, $V_{rev} = 64$ mV. **d**, Left panel: voltage dependence of the steady-state inactivation of wild-type $\text{Na}_v1.7$ plus β -subunits was measured by holding the membrane potential for 500 ms at conditioning voltages from -120 to 0 mV (at 5-mV increments) before stepping to a test pulse at -10 mV for 50 ms. The inset shows the voltage pulse protocol, which was applied at 0.5 Hz. Only the current responses to the test pulse are shown. Right panel: the peak currents obtained as on the left were normalized to the maximum peak current, and plotted against the holding potential applied during the conditioning pulse. The red line represents a fit of the data with a Boltzmann equation $y = (A_1 - A_2)/(1 + \exp((x - V_{0.5})/k)) + A_2$, where $V_{0.5} = -71$ mV, $k = 5.9$ mV, $n = 13$. Error bars in **c** and **d** represent standard errors.

their green fluorescence. Whole-cell voltage clamp recordings from cells co-expressing wild-type $\text{Na}_v1.7$ with the $\beta_1\beta_2$ subunits, revealed a voltage-gated Na^+ current with a peak amplitude of $-373 \pm 70 \text{ pA } \text{pF}^{-1}$ at -15 mV ($n = 13$), compared with a background current of $-3 \pm 1 \text{ pA } \text{pF}^{-1}$ ($n = 5$) in cells transfected with the $\beta_1\beta_2$ construct alone ($P = 0.005$ for wild-type $\text{Na}_v1.7$ versus control) (Fig. 4c). The voltage dependence of activation of $\text{Na}_v1.7$ could be described by a Boltzmann function, with half-maximum activation ($V_{0.5}$) of $-28 \pm 1 \text{ mV}$, $k = 4.9 \pm 0.5 \text{ mV}$ and a reversal potential (V_{rev}) of $+64 \pm 3 \text{ mV}$ ($n = 13$). Voltage-dependent inactivation could also be described by a Boltzmann function, with half-maximal inactivation at $-71 \pm 1 \text{ mV}$ and $k = 5.9 \pm 0.4 \text{ mV}$ ($n = 13$) (Fig. 4d). These properties, as well as the voltage dependence of the kinetics of activation and inactivation (Supplementary Fig. 1), are similar to those described previously for $\text{Na}_v1.7$ currents^{6,16–18}. In contrast, cells co-transfected with each of the mutated $\text{Na}_v1.7$ subunits plus $\beta_1\beta_2$ exhibited currents that were not significantly different from those recorded from control cells (Fig. 4c). The mean peak currents at -15 mV were: I767X, $-6 \pm 2 \text{ pA } \text{pF}^{-1}$ ($n = 7$, $P > 0.1$ versus control); W897X, $-5 \pm 1 \text{ pA } \text{pF}^{-1}$ ($n = 7$, $P > 0.2$ versus control); S459X, $-5 \pm 2 \text{ pA } \text{pF}^{-1}$ ($n = 5$, $P > 0.2$ versus control). These results indicate that the absence of pain in these patients is co-incident with a complete loss of function of $\text{Na}_v1.7$. Given the proposed role of $\text{Na}_v1.7$ in action potential generation in DRG neurons^{11,19,20} and the lack of pain perception in these patients, our data suggest that the firing of action potentials may be substantially compromised in nociceptive neurons lacking $\text{Na}_v1.7$. Although we favour a defect in peripheral nociceptive transmission as the most likely explanation for the lack of pain perception in these patients, we cannot rule out the possibility that the phenotype could be related to a $\text{Na}_v1.7$ -mediated central nervous system defect. SCN9A is known to be expressed in human⁸ and monkey²¹ spinal cord and brain, albeit at a much lower level than in dorsal root ganglia²¹.

Conclusions and prospects

SCN9A has previously been shown to be involved in nociception in both humans and rodents. The autosomal-dominant pain disorder primary erythermalgia (OMIM 133020), characterized by severe, episodic burning pain in the extremities in response to warm stimuli or moderate exercise, is caused by gain of function mutations in SCN9A ²². These mutations alter the threshold of activation of the $\text{Na}_v1.7$ sodium channel, resulting in hyperexcitability of pain signalling neurons^{16,23,24}. Loss of function mutations in $\text{Na}_v1.7$ have not been reported previously in humans, but have been studied in mice that lack $\text{Na}_v1.7$ in nociceptive neurons^{25,26}. Such mice show increased mechanical and thermal pain thresholds and striking deficits in the development of inflammatory pain symptoms. Global $\text{Na}_v1.7$ -null mutant mice, however, die shortly after birth²⁵, associated with a failure to feed, in stark contrast to the human families where there is no reported increase in early mortality. The amino acid sequences of human and mouse $\text{Na}_v1.7$ proteins are highly conserved (95% similarity and 92% identity, Supplementary Fig. 2), as is the domain structure. Why the global- $\text{Na}_v1.7$ -deficient mice should die when the humans do not is therefore unclear. It might, however, reflect species differences in early postnatal development or in the expression pattern or function of $\text{Na}_v1.7$ in non-nociceptive neurons.

Pain perception has evolved as a protective mechanism that allows an organism to detect tissue damage and then modulate its activity while repair occurs. This is illustrated by the nociceptive neuropathies ‘congenital insensitivity to pain with anhidrosis (HSAN4)’ (OMIM 256800) and ‘congenital insensitivity to pain (HSAN5)’, where affected individuals often suffer permanent injury during childhood because they fail to notice illnesses or injuries, and fail to learn pain-avoiding (severe risk-avoiding) behaviours—as in this study’s index case. Because pain perception pathways are so numerous and complex it was surprising that disruption of a single gene, SCN9A , would lead to a complete loss of nociceptive input. We show

here that this is the case, at least in humans. Given the key role of SCN9A in human pain perception, it is interesting to speculate whether single-nucleotide polymorphisms in SCN9A may explain variations in pain thresholds between individuals. Finally, as individuals with null mutations in SCN9A are otherwise healthy, drugs blocking $\text{Na}_v1.7$ function have the potential to produce new and potentially safer analgesia^{27,28}.

METHODS

Clinical note. We had originally diagnosed the study families as having congenital indifference to pain, but we subsequently found difficulty in the nomenclature of nociceptive disorders.

There are two schools of thought in the literature for distinguishing between congenital insensitivity to pain and congenital indifference to pain. On one side the distinction between insensitivity and indifference to pain is centred on the respective presence or absence of a neuropathy, this being the cardinal feature in insensitivity^{2,5}. The families we studied were diagnosed as having indifference owing to an absence of neuropathy in our patients. Also, the phenotype in our patients closely resembles that seen in other patients described with indifference: “not experiencing pain anywhere over their bodies from needle-prick or injury, but could recognize the point from the head of a pin, had no physiological responses to noxious stimuli, no evidence of neurological abnormality and biopsy and post-mortem examination did not disclose a structural abnormality of nerve, spinal cord or brain”².

On the other side the distinction outlines that indifference implies a lack of concern to a stimulus that is received and perceived (the sensory pathways are considered normal), whereas insensitivity describes the absence of painful sensation or failure to receive perception due to a detectable defect of sensory pathways³. From this point of view, the families in this study clearly have insensitivity, as they have no personal knowledge of pain.

The distinction between insensitivity and indifference can therefore be made on either histopathological grounds of finding a neuropathy, or on clinical grounds of whether the pain is felt and ignored or not felt at all; these approaches yield different diagnostic designations for our families.

The families reported here have no nociception (the ability to respond to tissue damage) and SCN9A null mutations. The problem is that loss of function of $\text{Na}_v1.7$ is a molecular defect that is not routinely detected by histopathology; that is, the patients have a normal nerve biopsy and so in the clinic they would probably be diagnosed as presenting with indifference rather than insensitivity to pain. However, the patients do not seem to fit the indifference diagnostic criteria of ‘detecting pain but not reacting to it aversively’. We therefore propose to call this disorder channelopathy-associated insensitivity to pain, which encompasses the underlying disease pathogenesis (a channelopathy affecting the nociceptive system) and the primary clinical feature (an inability to perceive nociceptive pain).

Microsatellite mapping and linkage analysis. Initial autozygosity mapping was performed using DNA samples from the affected individuals and their parents for families 1 and 2, and a panel of 400 polymorphic microsatellite markers, originally derived from the Weber Mapping Panel 6 and subsequently modified in-house. Family 3 was later similarly studied. The genotype data was analysed by hand for inconsistencies and by family haplotype to identify regions of homozygosity. To calculate a LOD score, the disease was analysed as an autosomal-recessive trait with a mutant allele frequency of 0.001, equal sex recombination frequencies and allele frequencies of $1/n$ (n = number of different alleles observed). Two-point LOD scores were calculated using MLINK from FASTLINK 5.1.

Novel polymorphic markers. All novel polymorphic markers were identified in genomic sequence by use of Tandem Repeats Finder and the UCSC Human Genome Browser. Primers were designed using Primer3 and checked for specificity by BLAST.

Mutation detection. All homozygous mutations were initially detected by bi-directional sequencing of genomic DNA using standard methods. Sequencing primers were designed using Primer3, BLAST and the sequence of AC107082 and AC108146. The mutations were confirmed to segregate in the families and to be absent from 150 ethnically matched human controls as follows: the family 2 (2298delT) and the family 3 (1376C→G) mutations were bi-directionally sequenced; amplification refractory mutation system (ARMS) polymerase chain reaction of the wild-type and mutant sequences was performed for the family 1 (2691G→A) mutation using the wild-type primer pair (5' to 3') TGCTTTACCTTGAACAAAAA and TGGAGAACGTGTTCATCTGC (product = 314 bp) and the mutant primer pair CTGTACGCTCCCACGGAGA and CATCACAAAATAATTCCACAGAGA (product = 224 bp).

Electrophysiology. HEK293A cells (QBiogene), cultured in DMEM supplemented with 5% FCS, were transiently transfected with plasmids expressing either wild-type or mutant *SCN9A* plus *DsRed2* and/or *SCN1B* plus *SCN2B* plus EGFP using lipofectamine 2000 (see Supplementary Methods for cloning). Experiments were performed 2–3 days after transfection on cells positive for *DsRed2* and EGFP (or EGFP for β-subunit only control). Fluorescence was detected with excitation at 550 ± 7 nm and 488 ± 5 nm, respectively, using appropriate emission filters and MetaMorph (Molecular Devices) software controlling a monochromator (Cairn) and a CCD-camera (Orca ER, Hammamatsu) mounted on an Olympus IX71 microscope with a ×40 objective. Microelectrodes were pulled from borosilicate glass (GC150T, Harvard Apparatus) and the tips coated with melted beeswax. Electrodes were fire-polished using a microforge (Narishige) and had resistances of 2.5–3 MΩ when filled with pipette solution. Standard whole-cell currents were filtered at 10 kHz and recorded at 20 kHz at 22–24 °C using an EPC10 amplifier controlled by patchmaster software (HEKA Electronic). The holding potential was –100 mV, 70% serious resistance compensation was used throughout, and currents were zero- and leak-subtracted using a p/4 protocol. Analysis was performed with pulsefit (HEKA Electronic) and Origin software (OriginLab Corp.). The bath solution contained (in mM): 3 KCl, 140 NaCl, 2 CaCl₂, 1 MgCl₂, 10 HEPES, 1 glucose (pH 7.4 with NaOH). The patch pipette solution contained (in mM): 107 CsF, 10 NaCl, 1 CaCl₂, 2 MgCl₂, 10 HEPES, 10 TEACl, 10 EGTA (pH 7.2 with CsOH).

Ethical and licensing considerations. The Cambridge Research Ethics Committee approved the study. There are no licensing considerations.

List of URLs. The UCSC Human Genome Browser is available at <http://genome.ucsc.edu/cgi-bin/hgGateway>;

Tandem Repeats Finder is available at

<http://tandem.bu.edu/trf/trf.submit.options.html>;

Primer3 is available at

<http://www-genome.wi.mit.edu/cgi-bin/primer/primer3-www.cgi>;

LALIGN is available at http://www.ch.embnet.org/software/LALIGN_form.html;

InterProScan is available at <http://www.ebi.ac.uk/InterProScan>;

FASTLINK 5.1 is available at <http://linkage.rockefeller.edu/soft/fastlink>;

BLAST is available at <http://www.ncbi.nlm.nih.gov/BLAST>.

Received 9 August; accepted 3 November 2006.

- Dearborn, G. A case of congenital general pure analgesia. *J. Nerv. Ment. Dis.* **75**, 612–615 (1932).
- Dyck, P. J. et al. Not 'indifference to pain' but varieties of hereditary sensory and autonomic neuropathy. *Brain* **106**, 373–390 (1983).
- Landrieu, P., Said, G. & Allaïre, C. Dominantly transmitted congenital indifference to pain. *Ann. Neurol.* **27**, 574–578 (1990).
- Nagashiko, E. M., Oaklander, A. L. & Dworkin, R. H. Congenital insensitivity to pain: an update. *Pain* **101**, 213–219 (2003).
- Klein, C. J., Sinnreich, M. & Dyck, P. J. Indifference rather than insensitivity to pain. *Ann. Neurol.* **53**, 417–418 (2003); author reply *Ann. Neurol.* **53**, 418–419 (2003).
- Klugbauer, N., Lacinova, L., Flockerzi, V. & Hofmann, F. Structure and functional expression of a new member of the tetrodotoxin-sensitive voltage-activated sodium channel family from human neuroendocrine cells. *EMBO J.* **14**, 1084–1090 (1995).
- Toledo-Aral, J. J. et al. Identification of PN1, a predominant voltage-dependent sodium channel expressed principally in peripheral neurons. *Proc. Natl Acad. Sci. USA* **94**, 1527–1532 (1997).
- Sangameswaran, L. et al. A novel tetrodotoxin-sensitive, voltage-gated sodium channel expressed in rat and human dorsal root ganglia. *J. Biol. Chem.* **272**, 14805–14809 (1997).
- Rush, A. M. et al. A single sodium channel mutation produces hyper- or hypoexcitability in different types of neurons. *Proc. Natl Acad. Sci. USA* **103**, 8245–8250 (2006).
- Amir, R. et al. The role of sodium channels in chronic inflammatory and neuropathic pain. *J. Pain* **7**, S1–S9 (2006).

- Cummins, T. R., Howe, J. R. & Waxman, S. G. Slow closed-state inactivation: a novel mechanism underlying ramp currents in cells expressing the hNE/PN1 sodium channel. *J. Neurosci.* **18**, 9607–9619 (1998).
- Amrani, N., Sachs, M. S. & Jacobson, A. Early nonsense: mRNA decay solves a translational problem. *Nature Rev. Mol. Cell Biol.* **7**, 415–425 (2006).
- Black, J. A. et al. Spinal sensory neurons express multiple sodium channel α-subunit mRNAs. *Brain Res. Mol. Brain Res.* **43**, 117–131 (1996).
- Catterall, W. A. From ionic currents to molecular mechanisms: the structure and function of voltage-gated sodium channels. *Neuron* **26**, 13–25 (2000).
- Isom, L. L. Sodium channel β subunits: anything but auxiliary. *Neuroscientist* **7**, 42–54 (2001).
- Cummins, T. R., Dib-Hajj, S. D. & Waxman, S. G. Electrophysiological properties of mutant Nav1.7 sodium channels in a painful inherited neuropathy. *J. Neurosci.* **24**, 8232–8236 (2004).
- Catterall, W. A., Goldin, A. L. & Waxman, S. G. International Union of Pharmacology. XLVII. Nomenclature and structure-function relationships of voltage-gated sodium channels. *Pharmacol. Rev.* **57**, 397–409 (2005).
- Herzog, R. I., Cummins, T. R., Ghassemi, F., Dib-Hajj, S. D. & Waxman, S. G. Distinct repriming and closed-state inactivation kinetics of Nav1.6 and Nav1.7 sodium channels in mouse spinal sensory neurons. *J. Physiol. (Lond.)* **551**, 741–750 (2003).
- Renganathan, M., Cummins, T. R. & Waxman, S. G. Contribution of Na(v)1.8 sodium channels to action potential electrogenesis in DRG neurons. *J. Neurophysiol.* **86**, 629–640 (2001).
- Blair, N. T. & Bean, B. P. Roles of tetrodotoxin (TTX)-sensitive Na⁺ current, TTX-resistant Na⁺ current, and Ca²⁺ current in the action potentials of nociceptive sensory neurons. *J. Neurosci.* **22**, 10277–10290 (2002).
- Raymond, C. K. et al. Expression of alternatively spliced sodium channel α-subunit genes. Unique splicing patterns are observed in dorsal root ganglia. *J. Biol. Chem.* **279**, 46234–46241 (2004).
- Yang, Y. et al. Mutations in *SCN9A*, encoding a sodium channel α subunit, in patients with primary erythermalgia. *J. Med. Genet.* **41**, 171–174 (2004).
- Dib-Hajj, S. D. et al. Gain-of-function mutation in Nav1.7 in familial erythromelalgia induces bursting of sensory neurons. *Brain* **128**, 1847–1854 (2005).
- Han, C. et al. Sporadic onset of erythermalgia: a gain-of-function mutation in Nav1.7. *Ann. Neurol.* **59**, 553–558 (2006).
- Nassar, M. A. et al. Nociceptor-specific gene deletion reveals a major role for Nav1.7 (PN1) in acute and inflammatory pain. *Proc. Natl. Acad. Sci. USA* **101**, 12706–12711 (2004).
- Nassar, M. A., Levato, A., Stirling, L. C. & Wood, J. N. Neuropathic pain develops normally in mice lacking both Nav1.7 and Nav1.8. *Mol. Pain* **1**, 24 (2005).
- Akopian, A. N., Abson, N. C. & Wood, J. N. Molecular genetic approaches to nociceptor development and function. *Trends Neurosci.* **19**, 240–246 (1996).
- Scholz, J. & Woolf, C. J. Can we conquer pain? *Nature Neurosci.* **5** (Suppl), 1062–1067 (2002).

Supplementary Information is linked to the online version of the paper at www.nature.com/nature.

Acknowledgements We thank the families who participated in this study, A. Boylston for critical advice, and Pfizer, the Wellcome Trust and St John's College, Cambridge for funding.

Author Contributions This study was designed by J.J.C., F.R., E.R., R.W., D.P.M., F.M.G. and C.G.W.; patient identification and phenotype assessment was performed by G.K., H.J., J.M., Y.R., L.A.-G., H.H., E.M.V., S.G. and C.G.W.; DNA extraction, linkage analysis, bioinformatics and sequencing was performed by J.J.C., A.K.N., E.R., K.S. and C.G.W.; cloning was performed by J.J.C.; electrophysiology was performed by F.R. and F.M.G.; and the paper was written by J.J.C., F.R., G.T., J.N.W., F.M.G. and C.G.W.

Author Information The sequence for full-length human *SCN9A* cloned from fetal brain mRNA is deposited in GenBank under accession number DQ857292. Reprints and permissions information is available at www.nature.com/reprints. The authors declare no competing financial interests. Correspondence and requests for materials should be addressed to C.G.W. (cw347@cam.ac.uk).